Calculation methods for radio pulses from high energy showers

J. Alvarez-Muñiz
Department of Physics, University of Wisconsin, Madison, Wisconsin 53706

R. A. Vázquez and E. Zas
Departamento de Física de Partículas, Universidade de Santiago, E-15706 Santiago de Compostela, Spain
(Received 22 March 2000; published 17 August 2000)

We present an approximation for the numerical calculation of Čerenkov radio pulses in the Fraunhofer limit from very high energy showers in dense media. We compare it to full Monte Carlo simulations in ice, studying its range of applicability, and show how it can be extended with a simple algorithm. The approximation reproduces well the angular distribution of the pulse around the Čerenkov direction. An improved parametrization for the frequency spectrum in the Čerenkov direction is given for phenomenological applications. We extend the method to study the pulses produced by showers at distances at which the Fraunhofer limit does not apply, and give the ranges of distances and frequencies in which Fraunhofer approximation is good enough for interpreting future experimental data. Our results are relevant for the detection of very high energy neutrinos with this technique.

PACS number(s): 96.40.Pq, 13.15.+g, 95.85.Bh, 96.40.Tv

I. INTRODUCTION

The confirmed detection of cosmic rays above the Greisen-Zatsepin-Kuz'min cutoff gives confidence in the existence of neutrinos of energies reaching the EeV scale and above. Such neutrinos are expected both in models in which the protons are accelerated to the highest energies [1], such as in active galactic nuclei [2] or gamma ray bursts [3] and in ''top bottom'' scenarios [4,5] in which cosmic rays are basically produced through quark fragmentation in events such as the decay of long lived heavy relic particles [6] or the annihilation of topological defects [7]. If the highest energy components of cosmic rays are protons, as suggested by increasing experimental evidence [8–10], they are expected to produce neutrinos in their interactions with the cosmic microwave background [11]. Neutrino detection would provide extremely valuable information on fundamental questions, both in astrophysics, such as the origin of the highest energy cosmic rays, and in particle physics.

Detecting high energy neutrinos may be a reality in the immediate future as many efforts are being made to develop large scale Čerenkov detectors under water or ice [12], designed to challenge the low neutrino cross section exploiting the long range of the high energy muons produced in charged current muon neutrino interactions. For EeV neutrinos these detectors are also capable of detecting light from high energy showers produced by neutrinos of any flavor in both neutral and charged current interactions, but the effective acceptance of the detector is reduced because the shower must be produced very close or within the instrumented volume.

It has been known for a long time that the development of showers in dense media produces an excess charge which generates a coherent Čerenkov pulse in the radiowave frequency when it propagates through the medium [13]. The detection of these pulses provides a possible alternative to neutrino detection particularly appropriate for very high energies [14–16] because the signal scales with the square of the primary energy [17,24]. The method is attractive because of the good transmission properties of large natural volumes of ice and sand and because much information about the charge distribution in the shower is preserved in the frequency and angular distribution of the pulses. This last property can be used to extract information about shower energy and neutrino flavor [18]. The technique faces a number of technical difficulties, however, [19] and several attempts are currently being made to test the theoretical predictions [20] and to study the feasibility of the technique in Antarctic ice [21].

Theoretical calculations are also difficult because a complete interference calculation calls for simulations capable of following electrons and positrons to the Čerenkov threshold ($\sim$100 keV). For high energy showers this is unfortunately out of the question because of the large number of particles involved and approximations have been specifically devised to study the radio emission of high energy showers in ice. The calculation of radio pulses from EeV showers has been possible in the *one dimensional* (1D) *approximation* which consists of neglecting both the lateral distribution and the subluminal velocity of shower particles [18,22,23]. All the calculations of radio pulses have been made so far in the Fraunhofer limit. In this limit the dependence of the electric field on the distance to the shower is trivial and the characterization of the angular distribution of the radio pulse at a given frequency is effectively only dependent on one variable, namely, the angle between the shower axis and the observation direction, which simplifies the simulations [24]. Clearly Fresnel type interference will take place if the showers are close enough to the detectors, but the calculation of these effects becomes even more time consuming.

In this paper we first give a brief introduction to coherent radio emission in Sec. II (fuller details can be found in Refs. [24,25]), accounting for the approximations made. In Sec. III we make extensive tests and explore the validity of the 1D approximation in the Fraunhofer limit by direct comparison with complete simulations, and we discuss the approxima-

tion, pointing out the connections between the radio emission and shower fluctuations, which gives new and useful insight into the radio emission processes. In Sec. IV we use the 1D approximation without taking the Fraunhofer limit to study the radio pulse as a function of the distance to the observation point. In Sec. V we summarize and conclude, commenting on the implications of our results for neutrino detection.

II. ČERENKOV RADIO PULSES

When a charged particle travels through a dielectric medium of refraction index n with speed βc greater than the phase velocity of light in that medium (c/n), then Čerenkov radiation is emitted in a frequency band over which the $\beta n > 1$ condition is satisfied without large absorption. The calculation of the Čerenkov electric field associated with the particle is a problem of classical electromagnetism that has been addressed elsewhere [26]. Solving the inhomogeneous Maxwell's equations in the transverse gauge, it is easy to obtain the Fourier components of the electric field produced by a current density $\vec{J}(\vec{x}',t')$:

$$\vec{E}(\vec{x},\omega)=\frac{e\mu_{\rm r}}{2\pi\epsilon_0 c^2}i\omega\int\int\int\int dt'd^3\vec{x}'\frac{e^{i\omega t'+ik|\vec{x}-\vec{x}'|}}{|\vec{x}-\vec{x}'|}\times\vec{J}_\perp(\vec{x}',t'), \quad (1)$$

where $\vec{J}_\perp(\vec{x}',t')$ is the component of the current transverse to the direction of observation $\vec{x}$. Also ν (ω) is the frequency (angular frequency), k is the modulus of the wave vector $\vec{k}$, μ_r is the relative permeability of the medium, and ϵ_0 and c are the permittivity and velocity of light in the vacuum.

A powerful approach to the simulation problem can be obtained by neglecting the lateral distributions in shower particles and assuming that all particles move at constant speed c in one dimension. We obtain a useful compact expression relating the charge distribution of the shower and its associated electric field. Crude as it may look, this approximation (1D approximation in brief) will be shown to give very good results particularly around the Čerenkov angle and it has allowed the possibility of establishing radio emission from EeV showers [22,23]. For simplicity we are going to take $\vec{x}'=\vec{z}'=z'\hat{n}_{z'}$ where $\hat{n}_{z'}$ is a unitary vector along the shower axis. The current associated with the shower development in this approximation is then given by

$$\vec{J}_\perp(\vec{z}',t')=Q(z')\,\vec{c}_\perp\,\delta^3(\vec{z}'-\vec{c}t'), \quad (2)$$

where $Q(z')$ is the longitudinal development of the excess charge in the shower. The substitution of this current into Eq. (1) leads to

$$\vec{E}(\vec{x},\omega)=\frac{e\mu_{\rm r}}{2\pi\epsilon_0 c^2}i\omega\sin\theta\,\hat{n}_\perp\times\int dz'\,Q(z')\frac{e^{i\omega z'/c+ik|\vec{x}-z'\hat{n}_{z'}|}}{|\vec{x}-z'\hat{n}_{z'}|}, \quad (3)$$

where θ is the angle between the shower axis and the direction of observation $\vec{x}$ and $\hat{n}_\perp$ is a unitary vector perpendicular to $\vec{x}$.

We can use this expression to obtain the Čerenkov electric field emitted by a particle shower propagating along a medium. Equation (3) accounts for the correct phase factors and distances for showers that are close to the observer (Fresnel region). In the Fraunhofer limit the phase factor in Eq. (3) can be approximated by $ik|\vec{x}-\vec{z}'|\simeq ikR-i\vec{k}\vec{z}'$, where $R=|\vec{x}|$ is the distance from the center of the shower to the observation point. It corresponds to the condition that the observation distance R exceed the Fresnel distance $R_F=\pi n\,\nu\,(L_s\sin\theta/2)^2/c$, where L_s is the typical length of the shower. In this limit it is straightforward to show that the electric field emitted by a shower in the 1D approximation can be related to the Fourier transform of the longitudinal charge distribution:

$$\vec{E}(\omega,\vec{x})=\frac{e\mu_{\rm r}}{2\pi\epsilon_0 c^2}i\omega\sin\theta\frac{e^{ikR}}{R}\hat{n}_\perp\int dz'\,Q(z')\,e^{ipz'}, \quad (4)$$

where we have introduced for convenience the parameter $p(\theta,\omega)=(1-n\cos\theta)\,\omega/c$ in Eq. (4) to stress the connection between the radio emission spectrum and the Fourier transform of the (excess) charge distribution. This allows a simple analogy to the classical diffraction pattern of an aperture function and helps the understanding of many of the complex features of the results obtained by simulation.

III. ONE-DIMENSIONAL APPROACH

We will explore the validity of the 1D approximation by direct comparison with simulation results in three dimensions. The program we use for the full simulation of electromagnetic showers in homogeneous ice is described in Ref. [24]. The results of the simulation will be compared to those obtained using Eq. (4) with different curves for the excess charge development function $Q(z)$, which will turn out to be quite illustrative.

Figure 1 compares the angular distributions of the pulses for showers initiated by different energy electrons using the full simulation and using Eq. (4) with $Q(z)$ directly from the excess charge depth distribution as obtained in the same simulations. Figure 2 displays the frequency spectra at different observation angles for a 10 TeV shower again for both approaches. Several conclusions can be drawn from these graphs with respect to the validity of the 1D approximation. Clearly the electric field amplitude around the Čerenkov cone is well reproduced in shape by the 1D approximation except in the Čerenkov direction where the approximation overestimates the amplitude by a factor that increases with frequency. Below 100 MHz the effect is negligible, becoming of order 20% (a factor of 2) for 300 MHz (1 GHz). The angular interval over which the approximation is valid slowly increases with shower energy and scales with the inverse of the frequency. Well outside the Čerenkov cone no agreement can be claimed but the order of magnitude of the approximation agrees with the simulation.

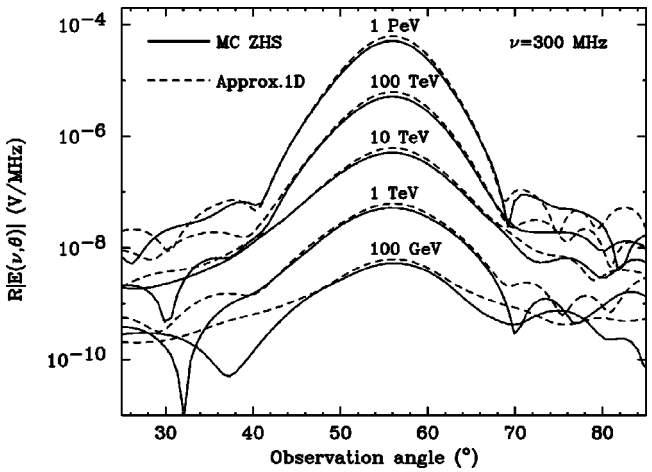

FIG. 1. Comparison of results of the 1D approximation to fully simulated pulses for electromagnetic showers of 100 GeV, 1 TeV, 10 TeV, 100 TeV, and 1 PeV. Simulations have been followed to threshold energy $E_{th}=1$ MeV. Shown is the angular distribution of the electric field amplitude for 300 MHz in the Fraunhofer limit multiplied by observation distance.

For completeness we give a new parametrization for the frequency spectrum in the Čerenkov direction using a finer subdivision of individual electron tracks (approximation *a*; see Appendix A), which represents a slight increase at frequencies above 500 MHz from that given in Ref. [24]:

$$R|\vec{E}(\omega,R,\theta_C)| \simeq 2.53\times 10^{-7}\left[\frac{E_{\rm em}}{1\ \ {\rm TeV}}\right]\left[\frac{\nu}{\nu_0}\right] \times\left[\frac{1}{1+(\nu/\nu_0)^{1.44}}\right]\ {\rm V\,MHz^{-1}}, \qquad (5)$$

where $\nu_0=1.15$ GHz. This parametrization is valid up to frequencies below ~5 GHz.

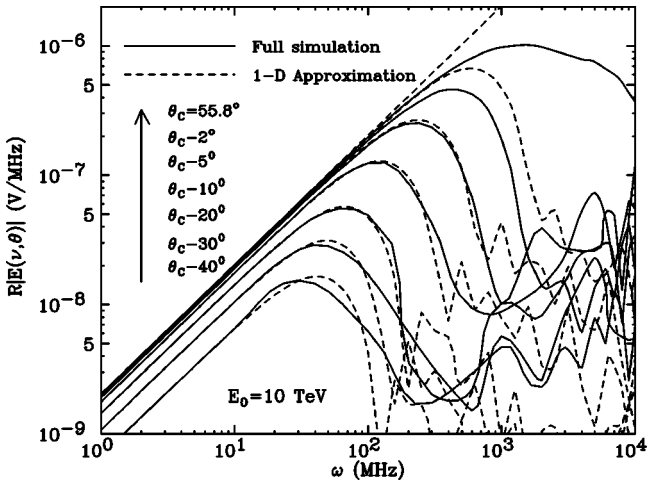

FIG. 2. Comparison of results of the 1D approximation to fully simulated pulses for a 10 TeV shower with $E_{th}=611$ keV. Shown is the frequency spectrum of the electric field amplitude for different observation angles.

It is worth discussing the interpretation of the behavior of this approximation before we attempt to understand its validity in more complicated showers such as those having strong Landau-Pomeranchuk-Migdal (LPM) effects [27,28]. In the Čerenkov direction, corresponding to $p=0$, the agreement between the approximation and the full simulation is excellent for frequencies below about 100 MHz. This corresponds to complete constructive interference characterized by a spectrum that increases linearly with frequency as shown in Fig. 2. Above 100 MHz the simulated frequency spectrum deviates from linear behavior because the wavelength becomes comparable to the transverse deviation of shower particles [24,29] and to a lesser extent because of time delays.[1] Both these effects are ignored in the 1D approximation, which keeps on rising linearly. Away from the Čerenkov cone the approximation becomes valid even to higher frequencies. Destructive interference in this case is due to the longitudinal excess charge distribution which is correctly taken into account by the approximation.

In spite of the approximation overestimating the amplitude of the electric field in the Čerenkov direction for frequencies above ~100 MHz, an *ad hoc* correction can be implemented based on the shape of the frequency spectrum as obtained in the simulations. Since this effect is due to the lateral distribution of the electromagnetic component of the showers, it can be corrected with a unique function for each frequency.

We have calculated the difference between the 1D approximation and the full simulation in the Čerenkov direction as a function of frequency, which is shown in Fig. 3 for two different shower energies. Note that the difference is (up to a factor that scales with shower energy) the same for showers of different energies. For this calculation we have actually improved the simulation by splitting the individual tracks in small subintervals (approximation *c*; see Appendix A). Also shown is the calculation without track subdivisions (approximation *a*) for comparison. The angular behavior of the correction at a particular frequency can be also shown to be fairly independent of energy.

The needed correction basically consists of rescaling the pulse just in the region around the Čerenkov direction. It can be achieved for instance dividing the result of Eq. (4) by a Gaussian correction factor (see Appendix B):

$$1+\left[\frac{S_{\rm 1D}\text{-}S_{\rm FS}}{S_{\rm FS}}\right]\exp\left(-\frac{1}{2}\left[\frac{\theta-\theta_C}{\sigma_\theta}\right]^2\right). \qquad (6)$$

The expression in brackets symbolically represents the relative difference between the frequency spectra as given by the 1D approximation ($S_{\rm 1D}$) and the full simulation ($S_{\rm FS}$) calculated in the Čerenkov direction. It simply sets the scale of the correction. The numerator is shown in Fig. 3 for two test

[1]It has been checked by direct simulation that the time delays only become important for frequencies in the 10 GHz range at the Čerenkov direction.

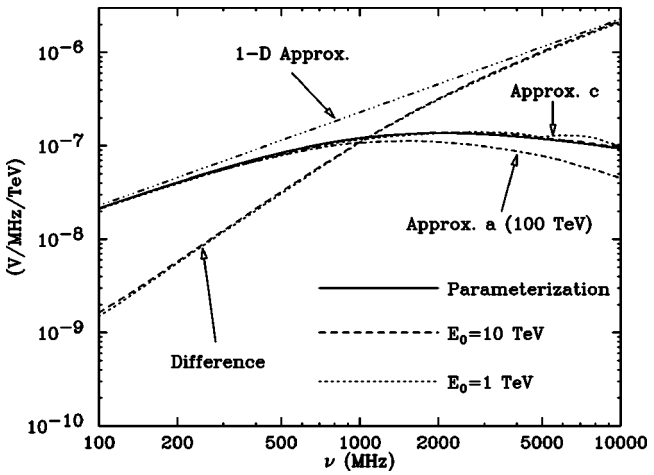

FIG. 3. Full simulation results for the frequency spectrum in the Čerenkov direction for 1 and 10 TeV electromagnetic showers in approximation *c* and for a 100 TeV shower in the standard approximation (*a*) used throughout for comparisons (see Appendix A). They are compared to the results using the 1D approximation (top curve). The improved parametrization for the *c* approximation given by Eq. (5) is also shown. The lower curves represent the difference between the 1D approximation and the full simulation results (using approximation *c*). Note that both the spectrum and the difference have the same behavior for all shower energies. All radio pulses scale with shower energy and are normalized to 1 TeV.

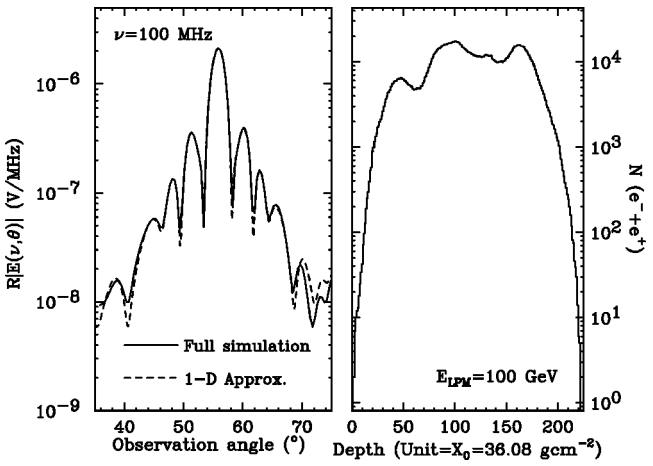

FIG. 4. Comparison of results of the 1D approximation to fully simulated pulses for a fictitious composite shower that combines two 10 TeV subshowers initiated at the origin and one 100 TeV subshower starting at a depth of 25 radiation lengths. Furthermore, these subshowers are artificially elongated by reducing the onset of the LPM effect (E_{LPM}=100 GeV instead of the actual value for ice which is 2 PeV). The longitudinal shower profile is also shown.

cases, showing that it also scales with energy at least in the energy interval checked. The half width of the Gaussian term is approximately given by

$$\sigma_\theta = 2.2^{\circ}\left[\frac{1\ \mathrm{GHz}}{\nu}\right]. \tag{7}$$

For frequencies above the 100 MHz scale and high energies when the full simulation is not viable, one would implement the correction by taking Eq. (5) instead of the full simulated result.

The 1D approximation also works for complicated showers such as those initiated by electrons and photons of EeV energies with strong LPM effects [22]. This has been explicitly checked by artificially lowering E_{LPM}, the onset energy for LPM effects, so that showers with energies that allow full three dimensional simulations display the characteristic LPM elongations [29]. The agreement between the full simulation and the 1D approximations is illustrated in Fig. 4 and it is clear that it is not limited to the central peak but also applies to the secondary peaks that appear in the angular distribution of the radiated pulse. This is expected since the lateral distribution of electromagnetic showers is similar for showers with and without the LPM effect [22,30]. The above correction prescription also works for these fictitious elongated showers with a mild reduction in precision.

Last, the simulation of the excess charge in an EeV shower can also be extremely time consuming because particles have to be followed at least to MeV energies when the interactions responsible for the excess charge become dominant over pair production and bremsstrahlung [24]. According to simulations the pulse scales with the excess track length and this is practically only due to an excess of MeV electrons. The excess number of electrons can be approximately obtained by rescaling the total number of electrons and positrons in a shower by the fraction of excess and total track lengths. This factor is very stable and has a value of 25% in ice [24].[2] As convenient parametrizations of the number of electrons and photons in showers are readily available it is possible to calculate shower size distributions for very large showers using them [22,23]. In spite of the small gradual rise in the excess charge as the shower develops shown by simulations [24], the effects of this approximation are mild, a slight narrowing of the pulse which is negligible compared to the other approximations made (see Fig. 5).

Finally it is remarkably fortunate that neglecting lateral distributions and time delays is a very good way of approaching the problem if some considerations are cautiously taken into account: namely, take the Fourier transform of the longitudinal distribution of the excess charge $Q(z)$ [or one-fourth of the total number of electrons and positrons if $Q(z)$ is not available] as given by Eq. (4); for frequencies above 100 MHz divide the 1D approximation by a correction factor as indicated by Eq. (6) taking Eq. (5) instead of the full simulation (S_{FS}) value.

Discussion: The relation between radio pulses and shower fluctuations

In the 1D approximation the Fourier transform for $p=0$ becomes the integral of $Q(z)$, i.e. the excess track length.

[2]This value corrects the previous conservative estimates used in [18], which quoted instead the ratio of excess projected track length to total track length as the relevant number (21%).

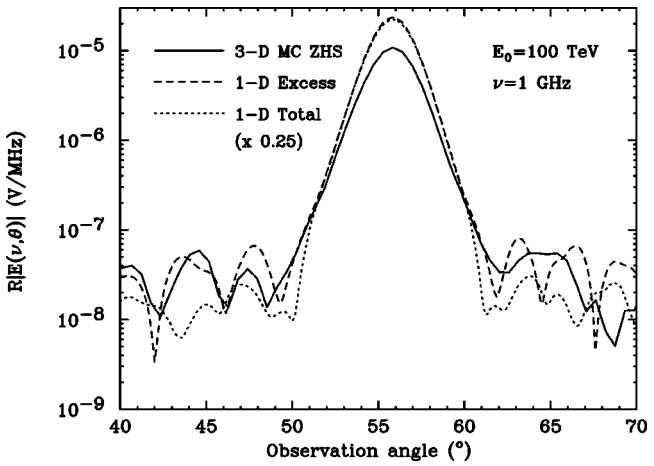

FIG. 5. Comparison of results of the 1D approximation to a fully simulated pulse for an electron shower of 100 TeV. Simulations have been followed to threshold energy $E_{th}=611$ keV. Shown is the angular distribution of the electric field amplitude for 1 GHz in the Fraunhofer limit multiplied by observation distance. Two curves are shown for the 1D approximation using the excess charge $Q(z)$ and the shower size $N(z)$ as obtained in the same simulation. The value obtained with shower size has been multiplied by 0.25 as explained in the text.

Simulations have shown that the excess track length scales extremely well with electromagnetic energy in the shower ($E_{\rm em}$) for both electromagnetic and hadronic showers up to energies exceeding 100 EeV with small fluctuations:

$$t=6400\left[\frac{E_{\rm em}}{1\ \ {\rm TeV}}\right]\ \ {\rm m}. \tag{8}$$

Incidentally this nice property of the excess charge together with the fact that the radio emission in the Čerenkov direction is proportional to the excess track length, makes such measurements excellent candidates for electromagnetic energy estimators.

A simple limit of the 1D approximation is obtained by taking an analytical expression for $Q(z)$ such as Greisen's parametrization for the average development of an electromagnetic shower [31]. The result just gives the radiation in the Čerenkov cone but no radiation outside, just like the Fourier transform of a Gaussian.

Invoking superposition we can subtract from a given shower development curve a smooth Greisen-like curve having the same track length. The result displays the ''roughness'' of the depth development curve and we shall refer to it as the *difference function*. The electromagnetic pulse is the sum of an isolated Čerenkov peak due to the Greisen-like curve and an extra contribution from the Fourier spectrum of the difference function which precisely vanishes at the Čerenkov direction because it does not contribute to the total track length. Moreover, for ordinary showers the amplitude of the difference function becomes smaller relative to shower size as the shower energy increases. This is just an statistical effect of having a larger number of particles and it indicates that the ''spatial correlations''[3] contained in the difference function must be related to fluctuations in shower size.

This effect can also be understood in terms of coherence. In the Čerenkov direction of greatest coherence the electric field amplitude scales with the shower energy E_0, but when the radiation is incoherent, i.e., well outside the Čerenkov direction, the electric field should add incoherently and hence scale with $\sqrt{E_0}$. This roughly agrees with simulations and nicely connects the properties of the radio emission to spatial correlations in shower development. Therefore the magnitude of the difference function becomes smaller relative to shower size as the shower energy increases, and the Čerenkov cone appears much more sharply ''illuminated'' with respect to directions outside the Čerenkov direction.

For LPM showers the structure of the pulse outside the central narrow peak is still dominated by the longitudinal development of these showers because the amplitude of the difference function is much larger than for a conventional shower. This is because LPM showers fluctuate a great deal. (One can picture a characteristic LPM shower as a superposition of smaller subshowers with typical smooth profiles with random starting points along the shower length.)

In other words, the Fourier modes of the excess charge distribution are probed by the electric field at a given value of p and hence at a given value of θ for a fixed frequency. The scale of the correlations in the distribution (the ''wavelength'' of the corresponding mode) is inversely proportional to p. As long as the scale of these correlations is larger than the characteristic lateral structure of the shower, the 1D approximation is expected to work. This is precisely what happens for the LPM fluctuations.

In summary there are two angular regions for the electromagnetic pulse with a not very well defined boundary. One angular region corresponds to the surroundings of the Čerenkov cone where the 1D approximation has powerful predictive power when one accounts for the correction described above. For the other region, outside the Čerenkov cone, the electric field amplitude drops considerably and behaves erratically, as some kind of ''white noise'' corresponding to the incoherent regime. In this region the short scale correlations of the excess track distribution are being probed and here the predictive power is lost with the approximations discussed. To calculate the radio pulse in such regions one needs three dimensional simulation programs which must sample tracks in small subintervals and which must follow all particles to the 100 keV region (approximation *c* described in Appendix A). All these requirements make it impossible with current computing power to simulate beyond 100 TeV. However, the region outside the Čerenkov cone, having much reduced radio emission, is not very relevant for shower detection.

[3]The name stresses the fact that they are different from standard fluctuations in shower theory because they refer to variations in shower size for the same shower at different positions rather than comparing shower size at the same spatial position for different showers.

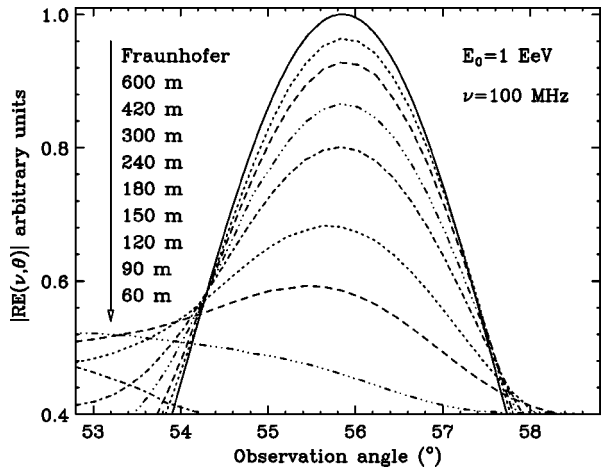

FIG. 6. Results of the 1D approximation as the observation distance approaches the Fresnel distance R_F for a 1 EeV electromagnetic spanning 135 radiation lengths.

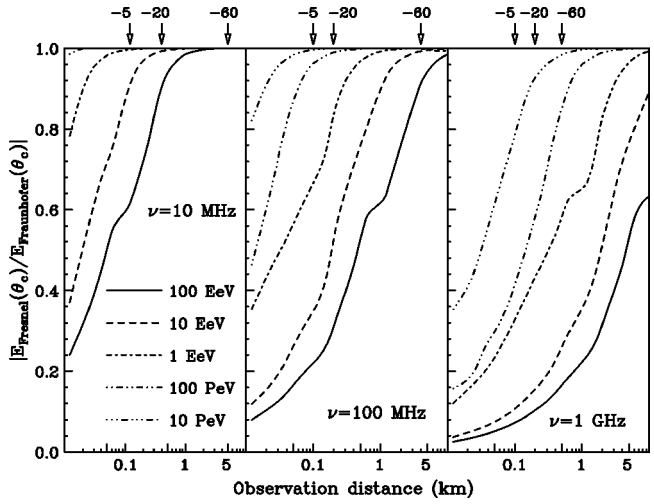

FIG. 7. Electric field amplitudes in the Čerenkov direction as a function of observation distance as obtained using the 1D approach for different frequencies. The amplitudes are normalized to the amplitude in the Fraunhofer limit. The arrows indicate the attenuation lengths for the corresponding frequencies at three different reference temperatures (in °C).

IV. VALIDITY OF THE FRAUNHOFER APPROXIMATION

All the previous radio pulse calculations have been made in the Fraunhofer approximation which corresponds to the limit

$$R > R_F = 3 \text{ m} \left[\frac{L_s}{1 \text{ m}}\right]^2 \left[\frac{\nu}{1 \text{ GHz}}\right]. \tag{9}$$

Taking $L_s \sim 3.8$ m, corresponding to the nominal ten radiation lengths in ice of an electromagnetic (hadronic) shower below about 10 PeV (10 EeV), a frequency of 1 GHz, and θ equal to the Čerenkov angle, then $R_F \sim 45$ m. This distance is to be compared with the km scale set by the small absorption coefficient of radio waves in cold ice; i.e., the Fraunhofer condition is clearly satisfied. For very long showers, such as those that display a very strong LPM effect, and high frequencies, R_F exceeds the typical attenuation scale. As the distance R is reduced to values below R_F, the diffraction pattern gradually turns into a Fresnel pattern in which the angular features become blurred.

It is possible to calculate diffraction patterns for such showers with the typical restrictions that apply to these simulations. A full calculation is again not viable for the shower energies at which this effect becomes important at km scale distances. We have calculated the radio pulses as observed at distances in which the Fraunhofer approximation breaks down, using simulated electron showers of different energies. We apply Eq. (3) for calculating electric field amplitudes at distances of order of the Fresnel distance R_F (a one dimensional transform that does not take the Fraunhofer limit). We calculate the effects for a range of energies and observation distances to specify the conditions under which the properties of the emission in the Fraunhofer limit are still valid.

In Fig. 6 we display the Čerenkov peak structure at 100 MHz for a range of distances around the Fraunhofer limit for a 1 EeV electromagnetic shower spanning 135 radiation lengths. We define the distance in relation to the center of charge of the shower. The calculated pattern has a reduced amplitude at the peak and becomes broader as expected. The Fraunhofer approximation is good to better than 10% in absolute value for distances above ~400 m. For a 100 EeV (10 PeV) shower the distance increases to 5 km (decreases to 20 m) for a roughly similar accuracy. The angular width of the pulse in the near field case increases with respect to the Fraunhofer case roughly by 20% when the amplitude reduces by 10%.

In Fig. 7 we plot the ratio of the calculated and Fraunhofer amplitudes at the Čerenkov peak as a function of distance to the shower for different frequencies and shower energies. Also indicated are the absorption lengths at three different temperatures for reference. This graph summarizes the results; for 1 km distance and energies above a few hundred PeV, Fresnel effects will become a serious concern for GHz frequencies. Provided that the distance to the shower and its direction can be determined, Fresnel effects could be corrected for, but this would clearly complicate and limit the analysis. This suggests that lower frequencies in the 100 MHz or even below may be appropriate for EeV showers. For hadronic type showers, however, no effects are foreseen for energies up to the 10 EeV range except for few abnormally long showers, which are unlikely to happen [23].

V. SUMMARY AND CONCLUSIONS

We have shown that the calculation of coherent Čerenkov radio pulses from high energy showers in ice in the Fraunhofer limit can be well approximated by neglecting the lateral distributions of the particles assuming that they travel at constant speed (c). The electric field amplitude simply becomes the one dimensional Fourier transform of the excess charge depth distribution. For the most relevant region around the Čerenkov direction, the approximation is correct for frequencies below 100 MHz. At higher frequencies the

approximation is still relatively good but systematically overestimates the pulse in the Čerenkov direction. We have shown that the model can be made to agree at least up to 1 GHz by subtracting a simple *ad hoc* Gaussian correction that is proportional to the shower energy and otherwise only dependent on frequency. We have reported the relevant parameters for the correction and have presented an improved parametrization for the electric field amplitude in the Čerenkov direction.

We have also shown that instead of the actual charge excess distribution one can use the shower size longitudinal development curve which is more conventional than the excess charge, scaling the amplitude of the central peak by the excess track length fraction 0.25.

We have developed a similar approximation for the region in which the Fraunhofer limit ceases to be valid. We have finally studied the behavior of the radio pulses of long electromagnetic showers in this region. Our results again suggest using low frequencies for EeV showers as concluded in Ref. [18]. These frequencies have a number of advantages because they are less attenuated, they allow observation of the angular structure with less detectors, and they have milder Fresnel effects at a given distance. Because of Fresnel corrections, the possibility of extracting the mixed character of electron neutrino interactions suggested in [18] requires frequencies below 100 MHz if the electron-initiated subshower exceeds about 10 EeV.

Lowering the frequency implies a higher threshold for detection because the Čerenkov spectrum increases with frequency but for EeV showers this should not be a problem. It has been estimated that the threshold for detecting showers at 1 km distance with 1 GHz broadband antennas is in the 10 PeV range [24]. Since the signal to noise roughly scales with the square root of the bandwidth which directly relates to the central frequency, a factor of 100 reduction in frequency will only call for about a factor of 10 enhancement of the threshold, still giving a very large signal to noise ratio for EeV showers.

Although our tests of the 1D approximation rely heavily on a specific simulation program [24], our claim on the validity of the 1D approximation is model independent. For testing purposes we used the charge excess distribution and the emitted radio pulses as obtained by the same routine. Numerically our results only apply for ice but it is only natural to expect that the same procedures can be applied to calculate the radiation in other materials.

ACKNOWLEDGMENTS

We thank P. Gorham for many early discussions about Fresnel corrections and D. Besson, D.W. McKay, J.P. Ralston, S. Razzaque, D. Seckel, and S. Seunarine for constructive criticism of the Monte Carlo calculations and many discussions. This work was supported in part by CICYT (AEN99-0589-C02-02) and by Xunta de Galicia (XUGA-20602B98). J.A. thanks the Department of Physics, University of Wisconsin, Madison and the Fundación Caixa Galicia for financial support. E.Z. thanks the Department of Physics, University of Wisconsin, Madison, where this work was finished, for its hospitality, and the Xunta de Galicia for partially supporting his trip.

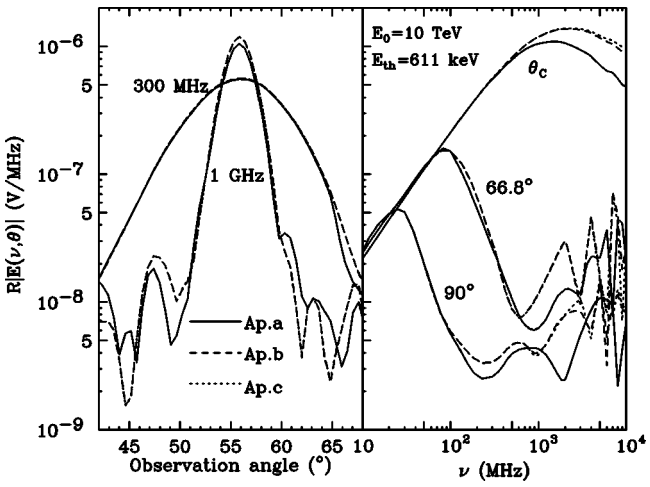

FIG. 8. Results of the full simulations with different algorithms for track subdivisions in the calculation of the electric field amplitudes as discussed in the text (Appendix A). Shown are both the angular distributions for 300 MHz and 1 GHz and the frequency spectrum at three different observation angles for a 10 TeV electron shower with a threshold of 611 keV.

APPENDIX A: THE ZHS MONTE CARLO CALCULATIONS

The simulation program used described in [24] is a specifically devised program for calculating radio pulses from electromagnetic showers that follows particles to $\sim$100 keV, taking into account low energy processes and timing. The depth development results have been compared to analytical parametrizations given by the Particle Data Group [32], with which they agree to a few percent. For the calculation of the radio emission from finite electron and positron tracks it uses the expression

$$\vec{E}(\omega,\vec{x})=\frac{e\mu_r i\omega}{2\pi\epsilon_0 c^2}\frac{e^{ikR}}{R}\vec{v}_\perp\left[\frac{e^{i(\omega-\vec{k}\cdot\vec{v})t_2}-e^{i(\omega-\vec{k}\cdot\vec{v})t_1}}{i(\omega-\vec{k}\cdot\vec{v})}\right], \tag{A1}$$

where $\vec{v}_\perp$ refers to the particle's velocity projected in a plane perpendicular to the observing direction and t_2 (t_1) is the time corresponding to the final (initial) point of the track. It can be obtained from Eq. (4) by replacing $Q(z)$ for a finite particle track. Several approximations can be made according to different choices in the subdivision of the individual charged particle tracks. In Ref. [33] three different choices, named approximations *a*, *b*, and *c*, have been compared, testing for convergence as the subtracks become smaller.

Approximation *a* is the standard that has been used in Refs. [24,34]. It corresponds to taking the end points of all the tracks, and it just uses the average velocity for the corresponding effective track in Eq. (A1). This is the standard reference calculation used throughout in this article except

for Fig. 3. Note that this approximation gives the correct result provided the particle velocity is constant along the track.

Approximation *b* subdivides the electron tracks according to the different interaction points found along the track (multiscattering is not considered as an interaction here). This approximation subdivides the track into finer subintervals as the energy becomes smaller, because the low energy electron scattering cross sections exceed bremsstrahlung and pair production. For each subtrack the average velocity is calculated between the corresponding end points of the track. Finally approximation *c* subdivides each interaction according to a convenient algorithm for splitting the propagation of particles designed to better calculate the multiple scattering at low energies.

The three approximations are compared in Fig. 8, illustrating the convergence of the method and how the approximation *a* is valid in the Čerenkov cone to a precision better than about 10% for frequencies below 1 GHz. Full simulations in approximation *c* are much more time consuming and have to be done for shower energies below ~100 TeV. At low energies fluctuations from shower to shower are more important so that these tests are inevitably subject to larger uncertainties because of such fluctuations.

APPENDIX B: THE GAUSSIAN APPROXIMATION

For electromagnetic (hadronic) showers below 10 PeV (10 EeV), that is, having no important deviations from Greisen behavior, the electric field around the Čerenkov cone can be accurately determined with a Gaussian approximation. The precise width of the cone inversely relates to the width (in z) of the excess charge depth distribution, $Q(z)$. As p is directly related to the observation angle θ with an expression that involves the frequency as an overall factor, the width of the angular distribution of the ''central peak'' becomes inversely proportional to ω.

For small deviations from the Čerenkov angle ($\Delta\theta$) the expression for p to first order is [18]

$$p=\frac{\omega}{c}\sqrt{n^2-1}\,\Delta\theta+O(\Delta\theta^2)\simeq 30.8\left[\frac{\nu}{1\ \mathrm{GHz}}\right]\Delta\theta\,(\mathrm{m}^{-1}). \tag{B1}$$

The numerical value given in this expression corresponds to showers in ice with $n=1.78$. Defining the Gaussian width by the points in which the amplitude drops by a factor $\sqrt{e}$ a Gaussian of half-width σ_z transforms to another Gaussian of half-width $\sigma_p=(\sigma_z)^{-1}$. We can fit a Gaussian to the excess charge depth development curve identifying the *shower length* by the width $l=2\sigma_z$ and the angular full width of the radiopulse is then

$$\sigma_\theta\simeq 3.72^\circ\left[\frac{1\ \mathrm{GHz}}{\nu}\right]\left[\frac{1\ \mathrm{m}}{l}\right] \tag{B2}$$

using approximation given by Eq. (B1). For a typical shower length of 8 radiation lengths (~3.1 m in ice) the angular width of the pulse is about 1° at 1 GHz, in agreement with Ref. [24].

[1] T.K. Gaisser, F. Halzen, and T. Stanev, Phys. Rep. **258**, 173 (1995).
[2] K. Mannheim, Astropart. Phys. **3**, 295 (1995).
[3] E. Waxman and J.N. Bahcall, Phys. Rev. Lett. **78**, 2292 (1997).
[4] V.S. Berezinsky, M. Kachelriess, and A. Vilenkin, Phys. Rev. Lett. **79**, 4302 (1997).
[5] P. Bhattacharjee and G. Sigl, Phys. Rep. **327**, 109 (2000).
[6] M. Birkel and S. Sarkar, Astropart. Phys. **9**, 297 (1998).
[7] P. Bhattacharjee, C.T. Hill, and D.N. Schramm, Phys. Rev. Lett. **69**, 567 (1992); R.J. Protheroe and T. Stanev, *ibid.* **77**, 3708 (1996).
[8] M. Ave, J.A. Hinton, R.A. Vazquez, A.A. Watson, and E. Zas (unpublished).
[9] F. Halzen, R.A. Vazquez, T. Stanev, and H.P. Vankov, Astropart. Phys. **3**, 151 (1995).
[10] D.J. Bird *et al.*, Phys. Rev. Lett. **71**, 3401 (1993).
[11] F.W. Stecker, C. Done, M.H. Salamon, and P. Sommers, Phys. Rev. Lett. **66**, 2697 (1991); **69**, 2738(E) (1992).
[12] AMANDA Collaboration, F. Halzen *et al.*, Nucl. Phys. B (Proc. Suppl.) **77**, 474 (1999); ANTARES Collaboration, C. Arpesella, Nucl. Instrum. Methods Phys. Res. A **409**, 454 (1998); BAIKAL Collaboration, talk presented at the 18th International Conference on Neutrino Physics and Astrophysics (Neutrino 98), Takayama, Japan, 1998; NESTOR Collaboration, in Proceedings of the XXVI International Cosmic Ray Conference, Salt Lake City, 1999, Vol. 2, p. 456.
[13] G.A. Askar'yan, Zh. Éksp. Teor. Fiz **41**, 616 (1961) [Sov. Phys. JETP **14**, 441 (1962)]; **48**, 988 (1965) [**21**, 658 (1965)].
[14] G.M. Frichter, J.P. Ralston, and D.W. McKay, Phys. Rev. D **53**, 1684 (1996).
[15] A.L. Provorov and I.M. Zheleznykh, Astropart. Phys. **4**, 55 (1995).
[16] P.B. Price, Astropart. Phys. **5**, 43 (1996).
[17] M.A. Markov and I.M. Zheleznykh, Nucl. Instrum. Methods Phys. Res. A **248**, 242 (1986).
[18] J. Alvarez-Muñiz, R.A. Vázquez, and E. Zas, Phys. Rev. D **61**, 023001 (2000).
[19] J.V. Jelley, Astropart. Phys. **5**, 255 (1996).
[20] P. Gorham, D. Saltzberg, P. Schoessow, M. Conde, W. Gai, J. Power, and R. Konecny, hep-ex/0004007.
[21] G.M. Frichter, in Proceedings of the XXVI International Cosmic Ray Conference [12], Vol. 2, p. 467; see also http://rice.bartol.udel.edu
[22] J. Alvarez-Muñiz and E. Zas, Phys. Lett. B **411**, 218 (1997).
[23] J. Alvarez-Muñiz and E. Zas, Phys. Lett. B **434**, 396 (1998).
[24] E. Zas, F. Halzen, and T. Stanev, Phys. Rev. D **45**, 362 (1992).
[25] H.R. Allan, *Progress in Elementary Particles and Cosmic Ray Physics* (North-Holland, Amsterdam, 1971), Vol. 10, p. 171.
[26] J.D. Jackson, *Classical Electrodynamics*, 2nd ed. (Wiley, New York, 1975).

[27] T. Stanev *et al.*, Phys. Rev. D **25**, 1291 (1982).
[28] S.R. Klein, Rev. Mod. Phys. **71**, 1501 (1999).
[29] J. Alvarez-Muñiz, Ph.D. thesis, University of Santiago de Compostela, Spain, 1999.
[30] J. Alvarez-Muñiz and E. Zas (in preparation).
[31] K. Greisen, in *Progress of Cosmic Ray Physics*, edited by J.G. Wilson (North-Holland, Amsterdam, 1956), Vol. III, p.1.
[32] Particle Data Group, C. Caso *et al.*, Eur. Phys. J. C **3**, 1 (1998).
[33] J. Alvarez-Muñiz, G. Parente, and E. Zas, in Proceedings of the XXIV International Cosmic Ray Conference, Rome, 1995, Vol. 1, p. 1023.
[34] F. Halzen, E. Zas, and T. Stanev, Phys. Lett. B **257**, 432 (1991).